

Investigations on the mechanical properties of hybrid nanocomposite hard coatings on polycarbonate

L. Sowntharya, S. Lavanya, G. Ravi Chandra, N.Y. Hebalkar, R. Subasri *

*International Advanced Research Centre for Powder Metallurgy and New Materials (ARCI), Balapur,
Hyderabad 500005, Andhra Pradesh, India*

Received 1 December 2011; received in revised form 31 January 2012; accepted 31 January 2012
Available online 10 February 2012

Abstract

Hybrid nanocomposite coatings derived from titanium tetraisopropoxide and epoxy or acrylic modified silanes were deposited on polycarbonate (PC) by dip coating employing various withdrawal speeds followed by ultraviolet and thermal curing. The effect of different organic functional groups in the precursors and ageing effect of these sols were systematically studied with respect to thickness, abrasion resistance, pencil scratch test, nanoindentation hardness and transmittance. The gels derived from the freshly prepared and aged sols were structurally characterized by FT-IR and TEM analysis. The viscosities of the sols were monitored with time. The change in viscosity is rapid for sol from epoxy modified silane. The thickness of the coatings increases with increase in viscosity in case of both the silane precursors. The scratch as well as abrasion resistance increases as a function of coating thickness. The pencil scratch hardness improves from 2B for the bare PC to a maximum of 3H for the coating obtained from an aged sol derived from epoxy modified silane. Also, the abrasion resistance of the coatings from same sol was maximum as evidenced by a <6% change in haze after 500 cycles, vis-a-vis 40% for the bare PC. The coatings from a freshly prepared sol of acrylic modified silane and titania showed the maximum nanoindentation hardness of 0.52 GPa, when compared to 0.23 GPa for the bare PC.

© 2012 Elsevier Ltd and Techna Group S.r.l. All rights reserved.

Keywords: A. Sol–gel process; B. Nanocomposites; C. Mechanical properties; E. Functional application

1. Introduction

The demand for transparent plastics has been on the increase in many industrial sectors. Due to its light weight, lower density and excellent optical clarity than glasses, many of the transparent polymeric materials such as polycarbonate (PC), polymethylmethacrylate (PMMA), and diallyl diglycol carbonate (CR-39) are being utilized to make windows, lenses or other optical devices [1]. Among them, PC possesses superior toughness and is an ideal material to replace glass components. Unfortunately, the lower abrasion resistance and poor scratch resistance cause a faster deterioration of the optical quality of the uncoated plastic [2]. In order to overcome the wear in plastics and to capitalize on their bulk properties, abrasion-resistant hard coatings have been developed over the past few

years using different techniques like gas phase, vacuum deposition (physical vapour deposition (PVD) [3], chemical vapour deposition (CVD) [4]) and sol–gel method [5–7].

Coating deposition on polymeric substrates is a big challenge because of their thermo-sensitive nature, and poor wettability/adhesion due to low surface free energy. The low cost and low temperature sol–gel process is the most interesting and viable alternative when compared to gas phase and vacuum-based techniques for coating deposition on plastics.

There are many reports highlighting the use of sol–gel organic–inorganic hybrid coatings on plastics [7–9]. Here, organic groups are incorporated into an inorganic backbone, formed by hydrolysis and condensation of silane precursors. These nanocomposite materials combine the properties like low temperature processing, light weight and good impact resistance of organic polymers with characteristics of inorganic oxides such as hardness, chemical stability and transparency [10]. The first step in this method is the preparation of the inorganic network during sol synthesis by hydrolysis and

* Corresponding author. Tel.: +91 40 24443567; fax: +91 40 24442699.

E-mail address: subasri@arci.res.in (R. Subasri).

condensation. In the second step, organic network is generated by thermal initiation or UV induced polymerization. The Si–C bond present in the organic–inorganic hybrid precursor is very stable and does not undergo hydrolysis. In order to enhance the physical properties, metal alkoxides of Ti [11], Zr, Al, etc. can also be incorporated into the nanocomposite sol.

The most common organically modified silicon precursors reported in the literature are methacryloxypropyltrimethoxysilane (MPTMS) [7,11] glycidoxypropyltrimethoxysilane (GPTMS) [12], vinyltrimethoxysilane (VTMS) [13], and vinyltriethoxysilane (VTES). Incorporation of Zr alkoxide into GPTMS [14] and MPTMS has been reported in literature. Soppera et al. [11] studied the chemistry of incorporation of Ti alkoxide in to MPTMS matrix. Philipp and Schmidt [15] studied the influence of titania, zirconia and silica alkoxide on synthesis and properties of epoxide group containing organically modified silicates. However, there is no systematic study reported on the effect of incorporating Ti alkoxide into different organically modified precursors on mechanical properties of coatings. Also, nanoindentation hardness studies on such coatings have not been reported. Conventionally, hardness is measured by pressing an indenter of a certain shape into the test surface and imaging the indent after releasing the load and retracting the indenter. However, when working with coatings, especially those with thickness of few microns, this method is not particularly convenient. Hence, an instrumented indentation technique, also known as nanoindentation is used, where the displacement of a sharp indenter into the test specimen is measured to probe into the mechanical properties of surfaces by accurately measuring displacements of only a few nanometer using sensitive transducers.

In the present investigation, organic-inorganic hybrid nanocomposite coatings were prepared using the two organically modified precursors, methacryloxypropyltrimethoxysilane (MPTMS) and glycidoxypropyltrimethoxysilane (GPTMS) along with titanium tetraisopropoxide. The obtained sols were dip coated on polycarbonate substrates. This paper reports the effect of different organic functional group of the matrix precursors and ageing of the two sols synthesized, on the mechanical and optical properties of the coatings.

2. Materials and methods

2.1. Chemicals

The reagents used were methacryloxypropyltrimethoxysilane (MPTMS, Gelest Inc., USA) and glycidoxypropyltrimethoxysilane (GPTMS, Gelest Inc., USA), titanium (IV) tetraisopropoxide (all of 97% purity, ABCR, GmbH, Germany), methacrylic acid (MAA, 99% purity, ABCR, GmbH, Germany), Isopropyl Alcohol (IPA, 99.7%, Qualigens fine chemicals, Mumbai, India), Isopropoxy ethanol (IPE, 99%, Aldrich, Germany), hydrochloric acid (HCl, Qualigens fine chemicals, Mumbai, India). MilliQ water was used for sol synthesis.

2.2. Sol synthesis

Two sols were prepared with different matrix precursors MPTMS and GPTMS in conjunction with titanium tetraisopropoxide precursor. In the first step, partial hydrolysis and condensation of the silane precursor was carried out by adding water and in presence of an acid catalyst (0.1 N HCl) and the mixture was kept for stirring. Due to the much higher reactivity of titanium (IV) isopropoxide, this component was complexed with methacrylic acid, which was slowly added to the prehydrolysed MPTMS/GPTMS under efficient stirring. The molar ratio of Si:Ti was 3.5:1. The sol was then kept for stirring for 24 h. The MPTMS-titanium (IV) isopropoxide (MT) and GPTMS-titanium (IV) isopropoxide (GT) sols were appropriately diluted prior to coating.

2.3. Coating and curing

The PC substrates were cleaned with 0.3% surfactant solution of Alconox[®] and then rinsed with distilled water and cleaned with IPA. The prepared MT and GT sols were dip coated on the cleaned 3 mm thick PC substrate of size 10 × 10 cm using different withdrawal speeds (1 mm/s, 3 mm/s and, 6 mm/s). One set of coatings was obtained from the freshly prepared MT and GT sol and the other set of coatings was obtained from the same sols subjected to ageing for 15 days. All the coatings were UV cured followed by thermal treatment at 130 °C for 1 h. UV curing of coatings on both sides was carried out using a three-medium-pressure-mercury lamp (120 W/cm with total wattage/lamp = 12 kW) conveyORIZED UV curing unit. The belt speed was maintained at 2 m/min during curing. The light dose as measured by UV radiometer (EIT Inc., USA) was 871 mJ/cm² in the UV-C region.

2.4. Characterization

The viscosities of the sols were determined prior to coating using viscometer (Anton Paar Rheolab QC, Germany, GmbH). The thickness of the coatings was measured using Thin-Film Analyzer using Filmetrics Inc F20, USA, which works on the reflectometry principle. This instrument measures the thin-film characteristics by reflecting and transmitting light through the sample, and then analyzing this light over a range of wavelength.

The scratch resistance of the coatings was determined by Wolff wilborn pencil tester GEF 720 N from Sheen instruments Ltd., as per ISO 15184; the scratched films were then analysed using optical microscope (Microstructure Olympus Bx51M).

The abrasion resistance of the coatings was measured by Taber abrader (Taber industries, 5155) using CS-10F wheel under 2 × 500 g load in accordance with ASTM D1044. The optical transmission of the coating was measured in the visible wavelength range using UV–VIS–NIR spectrophotometer (model: Varian Cary 5000i).

Nanoindentation studies were carried out using an MTS (now Agilent) Nanoindenter, model XP. As-coated samples were sliced into coupons of approximately 1 cm × 1 cm and

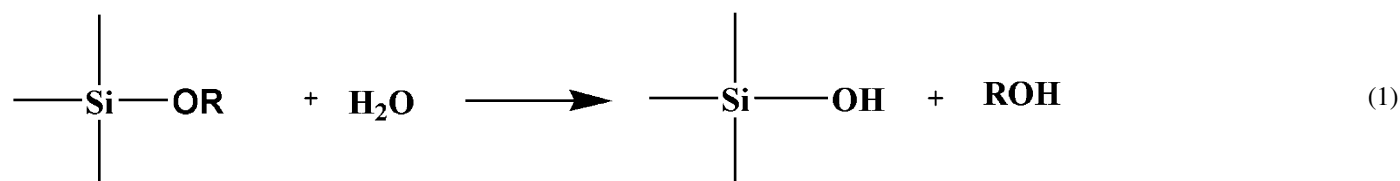
mounted on metal cylinders such that the coated surface faces the indenter, which were then inserted into the sample holder. All studies were carried out in the displacement-control mode. The continuous stiffness measurement (CSM) technique was used to measure the hardness and elastic modulus as a function of depth. The load at the final depth of indentation was held for duration of 30 s. Depending on the coating thickness, the samples were indented to depths of 500 nm, 1000 nm or 2000 nm, since it is generally accepted that when the depth of indentation is 1/10th or less of the coating thickness, the substrate effect can be avoided. However, all the analyses were carried out at 500 nm depth.

3. Results and discussion

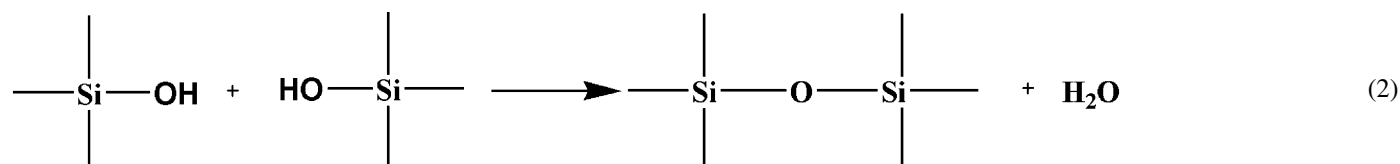
3.1. Reaction mechanism

The principal chemical reactions involved in the initial steps of sol–gel processing of inorganic and hybrid sol–gel materials are shown below. The hydrolysis (as shown in Eq. (1)) and condensation reaction leads to the formation of the inorganic network, as shown in Eq. (2).

Hydrolysis:

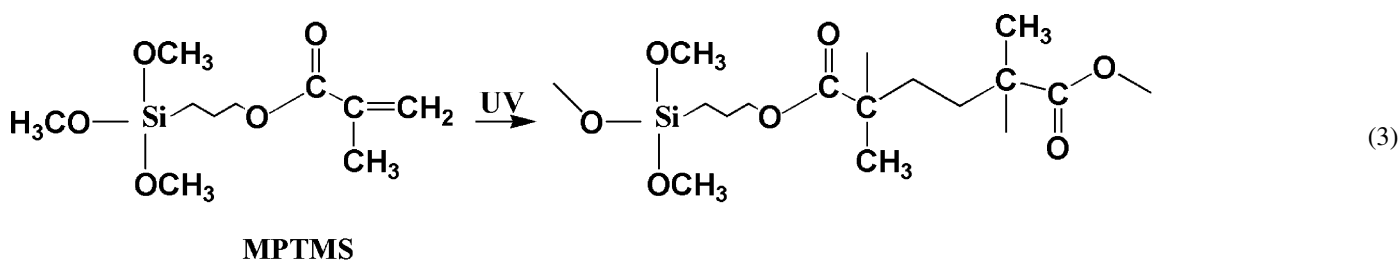


Condensation:



The Fourier-transformed infrared (FT-IR) spectra were recorded using Spectrum GX (Perkin Elmer, Singapore) spectrometer in the range 400–4000 cm^{−1}. The samples were mixed with KBr powder in the ratio 1:100. The fine powder was then compacted as a pellet and used for FT-IR studies. Transmission electron microscopy was carried out using Technai

In case of organically modified silane precursors with UV polymerizable functional groups, the organic group undergoes polymerization reaction in presence of UV radiation. The organic network formation in MPTMS and GPTMS are different. In case of MPTMS, only one polymerization pathway is possible as shown in Eq. (3).

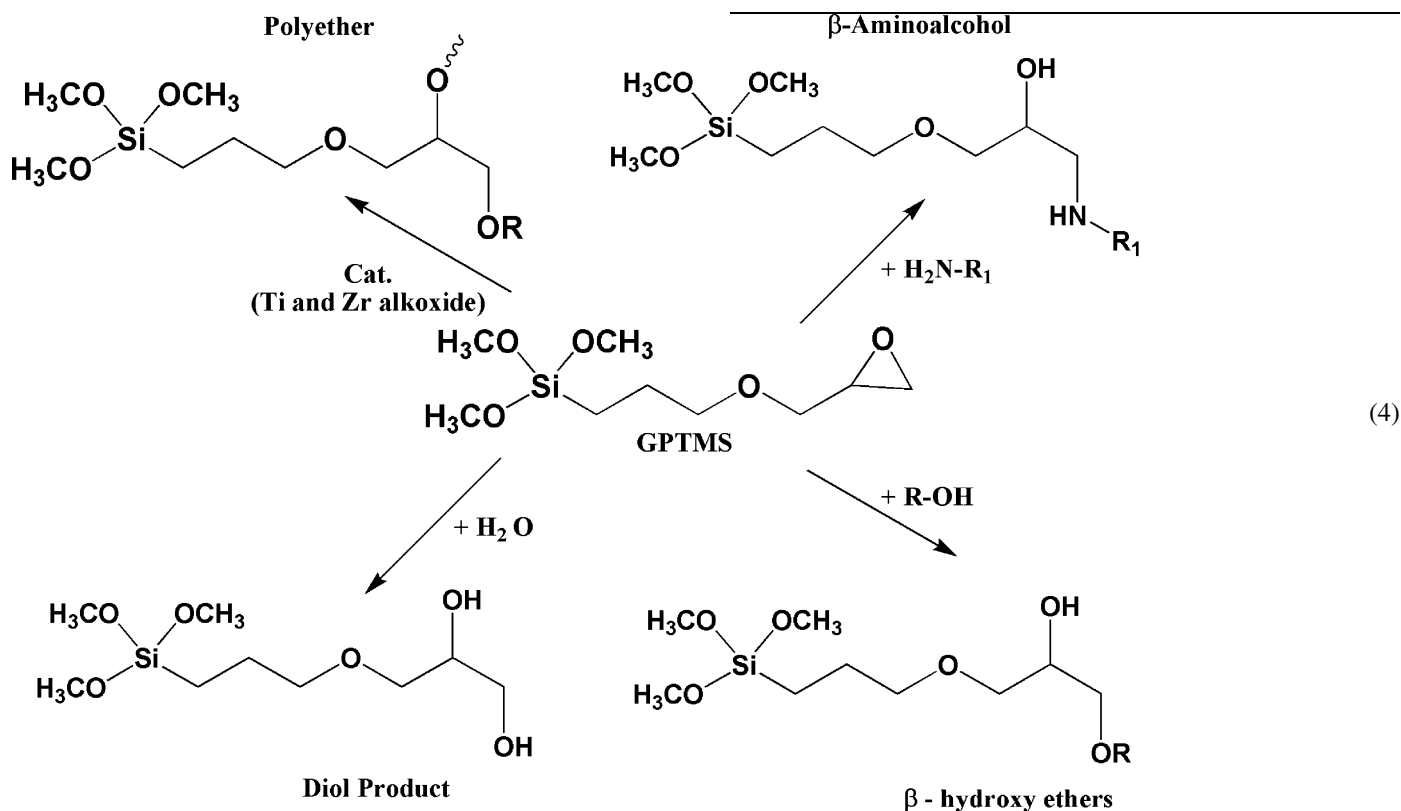


200 G2, FEI, Netherlands. A drop of the dispersion of powdered gel from aged GT sol, in 5 ml of ethanol was dispensed on a polymer coated copper grid and used for TEM analysis.

In case of GPTMS, the functional group present in the precursor can either undergo hydrolysis or alcoholysis or polyaddition reaction to form corresponding diol or β-hydroxy

ethers or polyether linkages respectively [12]. This scheme is shown below in Eq. (4).

set of coating was done after 15 days of ageing. The coatings were cured by UV radiation followed by thermal treatment.



Titanium tetraisopropoxide and zirconium n-propoxide acts as a catalyst for the polymerization of GPTMS to polyether [15]. Since in the present study, titanium tetraisopropoxide is used in sol synthesis, GPTMS is expected to undergo polymerization to form polyether. The titanium oxo-clusters resulting from partial hydrolysis of titanium alkoxide complexed with MAA can induce polymerization of organic monomers present in MPTMS [11] and GPTMS.

3.2. Effect of ageing on viscosity and thickness

The viscosities of the diluted MT and GT sol immediately after synthesis were found to be 4.7 and 17.5 mPa s respectively. After 15 days of ageing, the viscosity of the GT sol increased drastically to 104.8 mPa s and that of MT sol was 5.8 mPa s. The rapid increase in the viscosity of GT sol is due to fast polymerization of epoxy groups catalysed by titanium isopropoxide.

The effect of time on the thickness of the MT and GT sols was studied. Time plays a crucial role in case of GT sol. The viscosity of the sol was found to increase rapidly with time and hence the coating thickness also was found to increase. The first set of coating was done using freshly prepared MT and GT sol. Second

From Fig. 1, it was observed that for all withdrawal speeds, the thickness of the coating from aged sol was higher than the coatings obtained from freshly prepared sol i.e. the coating thickness also increases with time as the viscosity increases.

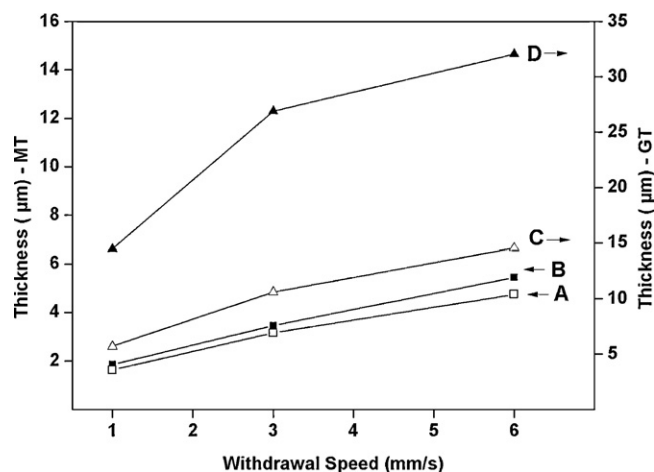


Fig. 1. Thickness vs. withdrawal speed for MT sol (A) coated using fresh sol (B) coated after 15 days ageing of the sol, and for GT sol (C) coated using fresh sol (D) coated after 15 days ageing of the sol.

Table 1
Pencil scratch test results for MT and GT sols.

Withdrawal speed (mm/s)	MT		GT	
	Freshly prepared	Aged for 15 days	Freshly prepared	Aged for 15 days
1	F	HB	HB	2H
3	F	F	F	3H
6	–	H	H	3H

The increase in coating thickness was much greater for the epoxy modified silane precursor, which indicates that the polymerization of the epoxy group was very fast and catalysed by the presence of metal alkoxide (titanium tetraisopropoxide) in the sol. The thickness of the coatings obtained from aged GT sol was very high; a coating with 30 μm thickness was also achieved using the aged GT sol without any crack after UV + thermal curing.

3.3. Pencil scratch and abrasion resistance

The results obtained for the pencil scratch test are shown in Table 1.

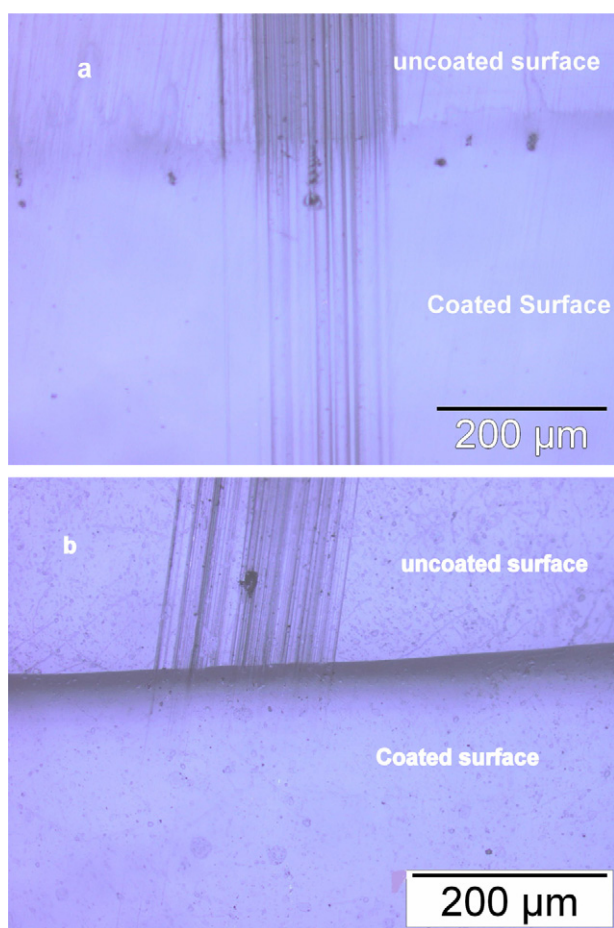


Fig. 2. Optical micrograph of surfaces after pencil scratch test on coatings withdrawn at 3 mm/s speed; the scratch direction is from top to bottom. (a) 2H pencil causing damage on coating from freshly prepared GT sol and (b) 2H pencil does not cause damage to the GT coating obtained after ageing the sol.

From Table 1 it is clear that the pencil scratch values of the coatings increases after ageing the GT sol for 15 days. This increase in the pencil scratch value is attributed to large increase in coating thickness of GT sol after ageing shown in Fig. 1. The variation of pencil scratch value as a function of coating thickness was studied by Linda et al. [16], who also reported that the pencil scratch increases with increasing thickness. The scratch on the coatings was examined using an optical microscope. Fig. 2a shows the image of the scratch on the coating surface (thickness 6 μm) from freshly prepared GT sol by 2H pencil, and for the same pencil, no scratch was observed on the coating surface (thickness 15 μm) obtained from the aged sol, as shown in Fig. 2b. The abrasion resistance of the uncoated and coated PC substrates was studied using Taber type abrader with CS-10F abrasion wheel under 2×500 g loading. The testing was done for 500 abrading cycles and after every 100 cycles the haze values were measured on different locations of the coated and uncoated areas on the wear track. The change in haze after abrasion is an indirect indication of the abrasion resistance of the coating. Since the MT and GT coatings from the aged sol yielded higher pencil scratch values as seen from Table 1, abrasion resistance was measured only for these coatings. It was found that GT showed a lower change in haze after abrasion and hence higher abrasion resistance as seen from Fig. 3. The results show that abrasion was also a function of thickness which was why the coating from GT sol showed higher abrasion resistance.

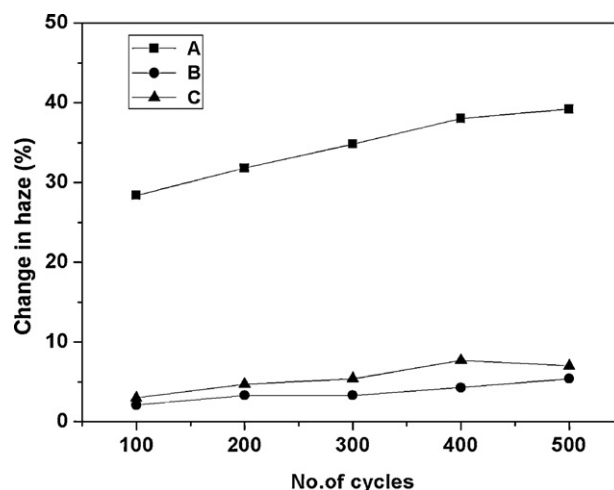


Fig. 3. Comparison of abrasion resistance of (A) bare PC with that of coatings obtained from aged sols (B) GT and (C) MT.

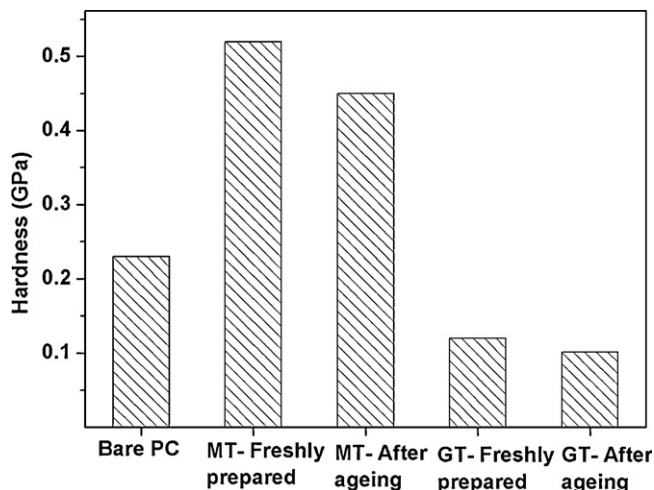


Fig. 4. Comparison of nanoindentation hardness values for bare and coated PC at a depth of 500 nm.

3.4. Nanoindentation

Nanoindentation measurements were carried out for GT and MT sol coatings obtained from the two sols. The hardness values obtained for different coatings are shown in Fig. 4. The

hardness of MT coatings was higher than that of PC for both the freshly prepared and aged sols, whereas in case of GT the hardness values were lower than that of PC. Since the inorganic network is common in case of both sols, the difference in hardness could be attributed to the different organic components. This is an indication that the polymerization product in case of MPTMS is harder than that formed in case of GT, which is a polyethylene oxide. Moreover, the hardness of both MT and GT sol was seen to have reduced for coatings from aged sols when compared to coatings from freshly prepared sol. This trend could be explained as due to the increase in the organic network for both coatings during ageing, which was also evident from the FT-IR studies, discussed in the next section. The highest nanoindentation hardness of 0.52 GPa was obtained for the MT coatings generated from a freshly prepared sol.

3.5. FT-IR analysis

Fig. 5a shows the FT-IR transmission spectra of the gels derived from MT and GT sols subjected to ageing over the spectral range 400–4000 cm^{-1} . The peaks arising from methacryloxy group of MPTMS are similar to that from methyl methacrylate [17].

A broad absorption band around 1110 cm^{-1} , 940 cm^{-1} , and one at 2900 cm^{-1} obtained can be assigned to Si–O–Si, Si–OH, and C–H bonds respectively [18]. The peak at 1635 cm^{-1} corresponds to acrylic group $\text{C}=\text{C}$. The low intensity of this peak indicates the progress of polymerization reaction in presence of UV radiation [16]. The peak at 1719 cm^{-1} corresponds to C=O stretching [18]. The peak at 3400 cm^{-1} corresponds to Si–OH. The intensity of this peak is low due to polycondensation of silanol group to form Si–O–Si bonds.

From the plot 2 of Fig. 5a, the presence of Titania particles is confirmed by the absence of absorption peak from

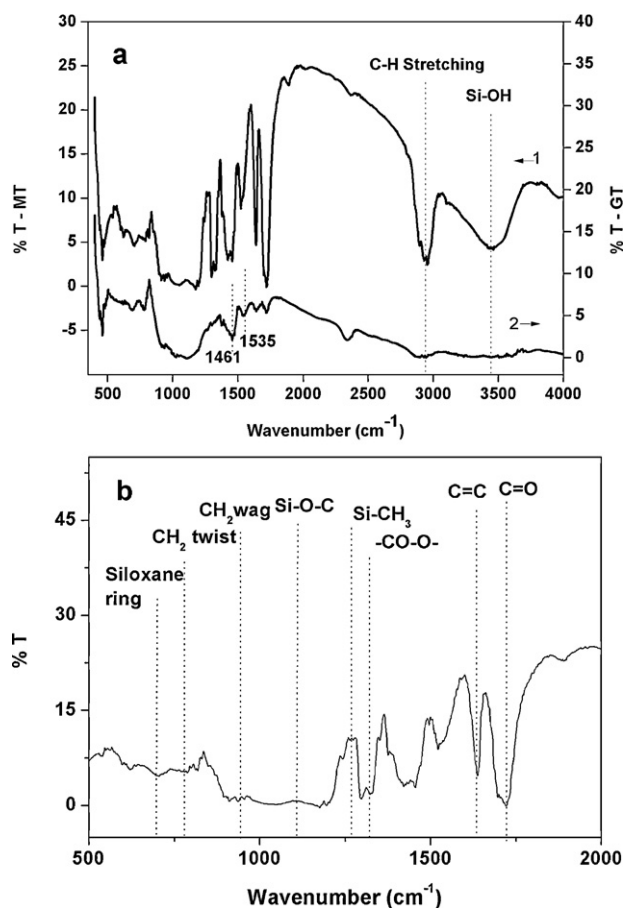


Fig. 5. FT-IR transmission spectra (a) over the spectral range 500–4000 cm^{-1} for gel derived from aged (1) MT sol and (2) GT sol; (b) over the spectral range of 500–2000 cm^{-1} for gel derived from aged MT sol.

Table 2

Assignment of the FT-IR peaks for MT and GT sols.

S. no.	Peak position (cm^{-1})	Assignment
1	694	Siloxane ring
2	650	Ti–O–Ti linkage
3	816	CH ₂ twist
4	938	Si–OH, CH ₂ wag
5	1089, 1100	Si–O–C stretch vibration, –Si–O–Si
6	1270	Si–CH ₂
7	1250–1300	<div style="text-align: center;"> $\begin{array}{c} \text{O} \\ \\ \text{---C---O---} \end{array}$ </div>
8	1428	skeletal vibrations
9	1635	CH ₂ Wag
10	1719	Bending of H ₂ O, C=C
11	2800–2900	C=O stretching
12	3461	C–H stretching
13	1461 and 1535	Si–OH
		Bidentate co-ordination between titanium centres and the carboxylic groups of MAA
14	2937	CH stretching

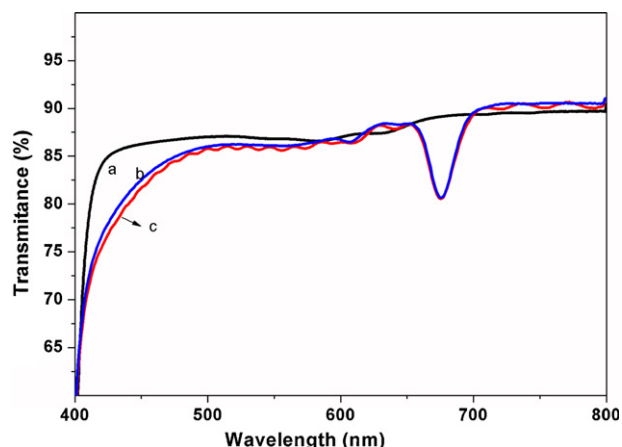


Fig. 6. Visible light transmittance spectra of (a) bare PC and PC coated with aged (b) GT sol (c) MT sol.

1400–1800 cm^{-1} . The epoxide group present in the siloxane is polymerized to polyethylene oxide (PEO). This can be confirmed by the absence of peaks at 910 and 853 cm^{-1} , which corresponds to epoxy vibrations [19,20]. The peak around 2900 cm^{-1} corresponds to $-\text{CH}-$ stretching. The FT-IR peak positions and assignment for MT and GT sol are given in Table 2.

3.6. Visible light transmittance

The transmittance spectra of the uncoated and coated PC measured over 400–800 nm wavelength range are shown in Fig. 6. The uncoated PC has an average transmission of 88% in the visible wavelength region. The average transmittance of MT and GT coatings from the aged sol is 84% below 700 nm and 90% above 700 nm.

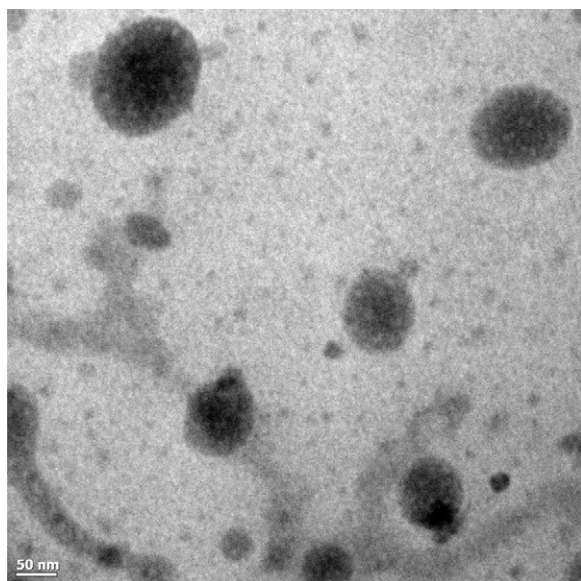


Fig. 7. Bright field TEM image of gel from aged GT sol.

3.7. Transmission electron microscopy

Fig. 7 shows the TEM image of the gel from aged GT sol. The appearance of nanosized particles having a different contrast to the matrix suggests that it is a nanocomposite material. The crystallinity of the nanosized phase however could not be unambiguously ascertained by electron diffraction imaging.

4. Conclusion

The characteristics of the precursors MPTMS or GPTMS in combination with titanium tetraisopropoxide for scratch resistance on polycarbonate substrates were systematically investigated. The effect of different functional groups in the matrix silane precursor and the ageing of the sol were studied with respect to the optical and mechanical properties of the coatings derived from these sols. The results of investigation showed that the viscosity of GT sol increased more rapidly with time than MT sol, due to which the shelf-life of GT sol was lower than that of MT. A linear correlation between the thickness and scratch as well as abrasion resistance of the coatings was observed. The maximum scratch and abrasion resistance was obtained for GPTMS-titania coatings obtained from aged sols. The nanoindentation hardness is an intrinsic property of the material and 0.52 GPa nanoindentation hardness was obtained for freshly prepared MPTMS-titania sol coating, which is the maximum value obtained among all the coatings studied in the present investigation. FT-IR analysis showed the difference in polymerization of the organic functional groups. TEM analysis confirmed the cured product to be a nanocomposite. Further investigations on varying ratios of silane: titanium tetraisopropoxide are in progress to optimize sol compositions that can yield coatings with best mechanical properties.

Acknowledgements

The authors gratefully acknowledge Dr. G. Sundararajan, Director ARCI and Dr. G. Padmanabham, Associate Director ARCI for providing constant support throughout the course of this investigation.

References

- [1] C. Li, K. Jordens, G.L. Wilkes, Abrasion-resistant coatings for plastic and soft metallic substrates by sol–gel reactions of a triethoxysilylated diethylenetriamine and tetramethoxysilane, *Wear* 242 (2000) 152–159.
- [2] N. Nakayama, T. Hayashi, Synthesis of novel UV-curable difunctional thiourethane methacrylate and studies on organic–inorganic nanocomposite hard coatings for high refractive index plastic lenses, *Prog. Org. Coat.* 62 (2008) 274–284.
- [3] S.V. Fortuna, Y.P. Sharkeev, A.J. Perry, J.N. Matossian, I.A. Shulepov, Microstructural features of wear-resistant titanium nitride coatings deposited by different methods, *Thin Solid Films* 377 (2000) 512–517.
- [4] R.J. Martin-Palma, R. Gago, V. Torres-Costa, P. Fernandez-Hidalgo, U. Kreissig, J.M.M. Duart, Optical and compositional analysis of functional

- SiO₂/CY: H coatings on polymers, *Thin Solid Films* 515 (2006) 2493–2496.
- [5] L.Y.L. Wu, G.H. Tan, X.T. Zeng, T.H. Li, Z. Chen, Synthesis and characterization of transparent hydrophobic sol–gel hard coatings, *J. Sol–Gel Sci. Technol.* 38 (2006) 85–89.
- [6] H. Schmidt, Transparent inorganic/organic copolymer by sol–gel process, *J. Sol–Gel Sci. Technol.* 1 (1994) 217–231.
- [7] S. Sepeur, N. Kunze, B. Werner, H. Schmidt, UV curable hard coatings on plastics, *Thin Solid Films* 351 (1999) 216–219.
- [8] T.H. Lee, E.S. Kang, B.S. Bae, Catalytic effects of aluminum butoxyethoxide in sol–gel hybrid hard coatings, *J. Sol–Gel Sci. Technol.* 27 (2003) 23–29.
- [9] M.A. Robertson, R.A. Rudkin, D. Parsonage, A. Atkinson, Mechanical and thermal properties of organic/inorganic hybrid coatings, *J. Sol–Gel Sci. Technol.* 26 (2003) 291–295.
- [10] G.M. Wu, J. Shen, T.H. Yang, B. Zhou, J. Wang, Hard UV-curable organo-mineral coatings for optical applications, *J. Mater. Sci. Technol.* 19 (2003) 299–302.
- [11] O. Soppera, Celine Croutxe-Barghorn, D.J. Loungnot, New insights into photoinduced processes in hybrid sol–gel glasses containing modified titanium alkoxide, *New J. Chem.* 25 (2001) 1006–1014.
- [12] G. Schottner, Hybrid sol–gel derived polymers: applications of multifunctional materials, *Chem. Mater.* 13 (2001) 3422–3435.
- [13] J. He, L. Zhou, M.D. Soucek, K.M. Wollyung, C. Wesdemiotis, UV-curable hybrid coatings based on vinylfunctionlized siloxane oligomer and acrylated polyester, *J. Appl. Polym. Sci.* 105 (2007) 2376–2386.
- [14] K. Luo, S. Zhou, L. Wu, High refractive index and good mechanical property UV-cured hybrid films containing zirconia nanoparticles, *Thin Solid Films* 517 (2009) 5974–5980.
- [15] G. Philipp, H. Schmidt, The reactivity of TiO₂ and ZrO₂ in organically modified silicates, *J. Non-Cryst. Solids* 82 (1986) 31–36.
- [16] Linda Y.L. Wu, E. Chwa, Z. Chen, X.T. Zeng, A Study towards improving mechanical properties of sol–gel coatings for polycarbonate, *Thin Solid Films* 516 (2008) 1056–1062.
- [17] S.K. Medda, D. Kundu, G. De, Inorganic–organic hybrid coatings on polycarbonate. Spectroscopic studies on the simultaneous polymerizations of methacrylate and silica networks, *J. Non-Cryst. Solids* 318 (2003) 149–156.
- [18] W.L. Walton, R.B. Hughes, Infrared spectra of α,β -unsaturated esters, *J. Am. Chem. Soc.* 79 (1957) 3985–3992.
- [19] G. De, D. Kundu, Silvert-nanocluster-doped inorganic–organic hybrid coatings on polycarbonate substrates, *J. Non-Cryst. Solids* 288 (2001) 221–225.
- [20] S.K. Medda, G. De, Inorganic–organic nanocomposite based hard coatings on plastics using in situ generated nano-SiO₂ bonded with (\equiv Si–O–Si–PEO) hybrid network, *Ind. Eng. Chem. Res.* 48 (2009) 4326–4333.